Eq. (1) in the case of hydrogen, where $\theta_0=850$, so that $\theta_0/\theta=2$:

$$(c/d)_H=30(\Delta E)^2(Mv^2)/(\hbar\omega_0)^3. \quad (9)$$

For deuterium this ratio should be roughly doubled.

Feldman *et al.* found values of 2.7×10^4 sec^{-1} for c and 9×10^6 sec^{-1} for d in the case of hydrogen, so that experimentally $c/d=3\times10^{-3}$ for hydrogen. For deuterium they found $d=8\times10^5$ sec^{-1}. The value of c was assumed to be unchanged, so that $c/d=3.4\times10^{-2}$ for deuterium.

Expressing all energies in multiples of Boltzmann constant, $\Delta E=0.44k$°K, $Mv^2=3\times10^4k$°K, and $\theta_0=850$°K for hydrogen, so that theoretically c/d should be 8×10^{-4} for hydrogen. For deuterium, where $\theta_0=640$°K, c/d should be 4.3×10^{-3}.

Thus the theory underestimates the ratio c/d by a factor 4 in the case of hydrogen and by a factor 8 in the case of deuterium. In other words, it overestimates the local-mode scattering by the same factors.

At first sight this lack of agreement is not encouraging. It should be noted, however, that spin-lattice relaxation times vary greatly as function of temperature and amongst species, and that this lack of agreement indicates at least a rough agreement in magnitude, particularly if it is noted that the coefficients d obtained from experiment are sensitive to the choice of θ_0, and thus uncertain by a factor of perhaps 1.5. Thus it is possible that the value of d for hydrogen and deuterium scale according to theory. Similarly, c depends sensitively on the choice of θ. Another uncertainty relates to the effective value of γ. Furthermore, the value of e_0^2 chosen here relates to the case of extreme localization of the local mode, i.e., when all the strain energy resides in one atomic cell. This is unlikely to be correct, and would lead us to overestimate d.

Nevertheless, there remains a discrepancy which most probably indicates that the theory of the anharmonic coupling of local modes to the acoustic branch[3] overestimates that interaction by a substantial numerical factor, possibly even as high as 10.

ACKNOWLEDGMENTS

The author wishes to thank his colleagues, Dr. Castle, Dr. Feldman, and Dr. Murphy for helpful discussions.

PHYSICAL REVIEW VOLUME 138, NUMBER 4A 17 MAY 1965

Paramagnetoelectric Effects in $NiSO_4\cdot6H_2O$†

S. L. Hou* and N. Bloembergen
Gordon McKay Laboratory, Harvard University, Cambridge, Massachusetts
(Received 28 December 1964)

Piezoelectric paramagnetic crystals can show a linear dependence of the paramagnetic susceptibility on an applied electric field. This effect has been detected in $NiSO_4\cdot6H_2O$ at low temperatures. The thermodynamic inverse effect, the creation of an electric polarization by applied magnetic fields, has also been observed. Both effects are derived from a free energy which for the tetragonal 422 symmetry takes the form $\xi(H_aE_b-H_bE_a)H_c$, where c denotes the tetragonal axis. The quantity ξ has been measured as a function of temperature. It has a pronounced maximum at 3°K, where $\xi=2.6\times10^{-9}$ esu. It passes through zero at 1.38°K. Between 10 and 70°K it decreases approximately as T^{-2}. These features are explained by a microscopic theory which considers the linear variation in an applied electric field of all parameters in the spin Hamiltonian of the four Ni^{++} ions in the unit cell. The dominant contribution comes from the change in the crystal-field splitting D.

I. HISTORICAL INTRODUCTION

THE influence of an electric field on magnetic properties and the influence of a magnetic field on dielectric properties was an important question in the early days of quantum mechanics.[1] Experiments[2] on gaseous NO showed the absence of such magnetoelectric cross effects. A simple physical explanation was suggested by de Haas. Orientation of electric dipole moments induces a spatial preference for the molecules to be pointing either up or down, but does not establish a preference for clockwise or counterclockwise rotation. Modern quantum mechanics soon afterwards provided a more rigorous basis for this suggestion.[1] The proof is, however, based on the fact that the partition function Z or the thermodynamic potentials cannot have terms E^sH^t, with $s+t$ odd. This is not true in systems lacking inversion symmetry. It is interesting to note that Huber,[2] guided by the qualitative considerations of de Haas, made an attempt 40 years ago to detect the

† This research was supported jointly by the U. S. Office of Naval Research, the Signal Corps of the U. S. Army and the U. S. Air Force. A preliminary account was given in Bull. Am. Phys. Soc. 9, 13 (1964). More detailed information than could be presented in this paper may be found in the Ph.D. thesis of S. L. Hou, Harvard University, 1964 (unpublished), or in Cruft Laboratory Technical Report 458, Harvard University (unpublished).

* Present address: Corning Glass Works, Corning, New York.

[1] See J. H. van Vleck, *Theory of Electric and Magnetic Susceptibilities* (Clarendon Press, Oxford, England, 1932), pp. 113–118, 279–281.

[2] A. Huber, Z. Physik **27**, 619 (1926).

effect in piezoelectric crystals of $NiSO_4 \cdot 6H_2O$ and $NiSeO_4 \cdot 6H_2O$. He obtained a negative result, but he might have found the effect reported in this paper, if he had extended his measurements to liquid-helium temperatures.

Some 30 years later Landau and Lifshitz[3] observed that the Shubnikov groups permit the existence of certain magnetic crystal classes with a term in the free-energy proportional to EH. Dzyaloshinski pointed out that antiferromagnetic Cr_2O_3 belongs to such a class. Astrov[4] and Rado[5] demonstrated experimentally the existence of magnetoelectric effects in Cr_2O_3.

The existence of a term in the free-energy proportional to EH^2 in piezoelectric paramagnetic crystals was first pointed out by Bloembergen.[6] He arrived at this conclusion along an independent historical path. Between 1950 and 1960 there had been several unsuccessful attempts to detect the influence of an applied electric field on magnetic resonance spectra. An observable effect, linear in the applied electric field, can however be expected whenever the magnetic ion or nuclear spin is located at a site which lacks inversion symmetry.[7] In this case all constants in the spin Hamiltonian become linear functions of the applied electric field. Because the paramagnetic susceptibility is a function of these parameters in the spin Hamiltonian, it in turn becomes a function of the electric field strength E. If the crystal as a whole lacks inversion symmetry, it can be a linear function of E. Since the relative variation of the parameters in the spin Hamiltonian is typically[8,9] $E/E_{at} \approx 1:10^8$ to $1:10^9$ for $E=1$ V/cm, a similar relative variation in χ may be expected. It was predicted[6] that the effect should be readily detectable in $NiSO_4 \cdot 6H_2O$ at low temperatures for $E \sim 10^4$ V/cm.

The experimental apparatus and results are described in the next section. A review of the magnetic structure derived from specific-heat and susceptibility data is given in Sec. III. The microscopic theory of the paramagnetoelectric (PME) effect is given in Sec. IV. A comparison with experimental data is given with special emphasis on temperature dependence. In the concluding section a comparison with the magnetoelectric effect in antiferro- and ferromagnetic materials is made. Rado[10] has given analogous macroscopic and microscopic interpretations for the effect in antiferromagnetic Cr_2O_3.

II. EXPERIMENTAL METHOD AND RESULTS

The PME effect can quite generally be derived from a thermodynamic potential

$$F_{\mathrm{PME}} = -\xi_{ijk}\mathcal{E}_i H_j H_k. \tag{1}$$

The electric field is denoted by $\mathcal{E}$ to avoid confusion with the spin-Hamiltonian parameter E. A summation over the three indices is understood. The third-rank tensor ξ is symmetric in the last two indices and has the same symmetry properties as the piezoelectric tensor.

$NiSO_4 \cdot 6H_2O$ belongs to the crystal class with point-group symmetry D_4 or 422. In this case the only nonvanishing elements of the third-rank tensor are $\xi_{14} = -\xi_{25} = \xi$. The PME thermodynamic potential takes the form

$$F_{\mathrm{PME}} = -\xi(\mathcal{E}_a H_b - \mathcal{E}_b H_a) H_c. \tag{2}$$

Here c denotes the tetragonal (screw) axis and a and b denote the other two principal directions of the tetragonal unit cell.

The existence of this term may be demonstrated experimentally in several ways. Application of a large dc magnetic field H_c along the tetragonal axis and a smaller oscillating field $h \cos\omega_m t$ at right angles anywhere in the ab plane will result in a magnetically induced electric polarization, perpendicular to both H_c and h, with a magnitude $P_{\mathrm{PME}} = +\xi h H_c \cos\omega_m t$. Conversely, the application of H_c and an oscillating electric field $\mathcal{E} \cos\omega_m t$ anywhere in the ab plane will result in an induced magnetization, perpendicular to both H_c and $\mathcal{E}$, with a magnitude $M_{\mathrm{PME}} = \xi \mathcal{E} H_c \cos\omega_m t$. The quantity $\xi\mathcal{E}$ may be regarded as the electric-field-dependent part of the magnetic susceptibility.

A. Electric Polarization Induced by Magnetic Fields

A single crystal of $NiSO_4 \cdot 6H_2O$ supplied by Semi-elements Inc. was mounted in the tail of a glass helium Dewar between the pole pieces of an electromagnet as shown in Fig. 1. The crystal has retangular dimensions, 0.077 in. × 0.352 in. × 0.350 in., where the last dimension is along the c axis. Silver electrodes are painted on the broad square faces. A phosphor bronze spring holds the crystal and connects the bottom electrode to the grounded outer conductor of a coaxial line. The other electrode terminates the inner conductor of this line which is connected to the input of a Keithley 603 Electrometer Amplifier.

An ac magnetic field is provided at right angles to H_c by two modulation coils, consisting of 720 turns of 24-

[3] L. D. Landau and E. M. Lifshitz, *Electrodynamics of Continuous Media* (Addison-Wesley Publishing Company, Inc., Reading, Massachusetts, 1960), pp. 116–119.

[4] D. N. Astrov, Zh. Eksperim. i Teor. Fiz. **38**, 984 (1960); **40**, 1035 (1961) [English transls.: Soviet Phys.—JETP **11**, 708 (1960); **13**, 729 (1961).]

[5] V. J. Folen, G. T. Rado and E. W. Stalder, Phys. Rev. Letters **6**, 607 (1961); G. T. Rado and V. J. Folen, *ibid.* **7**, 310 (1961).

[6] N. Bloembergen, in *Proceedings of the International Conference on High Magnetic Fields*, edited by B. Lax (John Wiley & Sons, Inc., New York, 1962), p. 454.

[7] N. Bloembergen, Science **133**, 1363 (1961).

[8] N. Bloembergen, *Proceedings of the XI Colloque Ampere*, edited by J. Smidt (North-Holland Publishing Company, Amsterdam, 1963), p. 39.

[9] See, for example, E. B. Royce and N. Bloembergen, Phys. Rev. **131**, 1912 (1963).

[10] G. T. Rado, Phys. Rev. Letters **6**, 609 (1961); Phys. Rev. **128**, 2546 (1962).

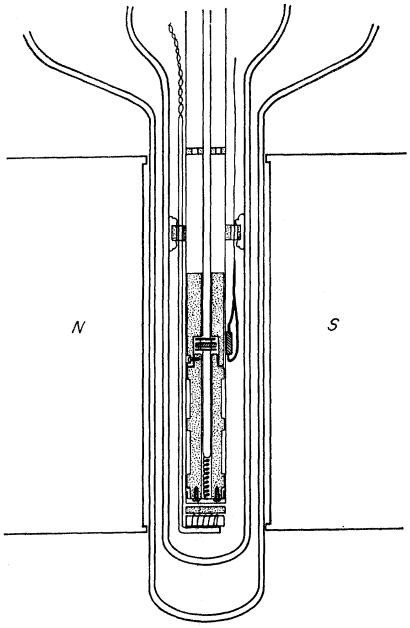

FIG. 1. Apparatus for measuring the electric polarization induced by magnetic fields. The modulation coils for the second magnetic field are not shown. The sample holder material, shown as the dotted area, is made of Teflon.

gauge copper wire each, mounted outside the cryostat between the pole pieces. A 75-W audioamplifier can produce a peak-to-peak modulation of 180 G at 30 or 50 cps. Another pair of modulation coils wound around the pole caps can provide a modulation field h parallel to H_{dc}.

The temperature of the sample can be varied between 4.2 and 1.28°K by pumping on the helium vapor. The lowest temperature corresponds to a pressure of 1.07-mm Hg, obtained by a CVM-556 Kinney pump with a 2-in. pump line. Vibrations of the pump were minimized by a rubber coupling section ($2\frac{3}{4}$ in. o.d.) loaded with 100 lb of brass. A Hg and oil manometer served to measure the temperature in this range. The pressure is regulated by a valve. The temperature can be raised above 4.2°K after the helium is evaporated by a heater. It takes about 11 h for the apparatus to warm up from 4.2 to 77°K, if no current is applied to the heater. The temperature is monitored by a carbon resistor between 4.2 and 20°K and by a platinum standard resistance thermometer between 20 and 77°K. A Leeds and Northrup K-2 potentiometer is used to measure the resistance.

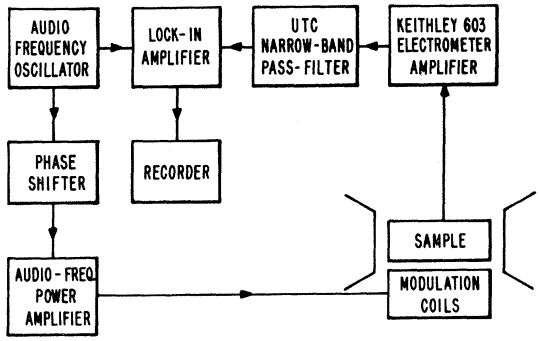

FIG. 2. Block diagram for the detection of the PME effect.

The induced electric polarization in the crystal of area A is equivalent to a current source

$$I_s = dq/dt = AdP/dt = i\omega_m AP$$

which feeds into a parallel combination of the impedance presented by the crystal and the input impedance of the Keithley electrometer amplifier. The input resistance of the amplifier is $R_i = 10^{14}\Omega$. The leakage resistance of the crystal is $R_c > 10^{12}\Omega$. Since the input capacitance is $C_i = 10$ pF and the capacitance of the crystal plus the coaxial line is $C_c = 75$ pF, the input admittance is $\omega_m(C_i+C_c) \gg R_i^{-1}+R_L^{-1}$ for modulation frequencies larger than 10 cps. The input voltage is therefore independent of ω_m, as verified experimentally,

$$V_s \approx AP/(C_i+C_c)\,.$$

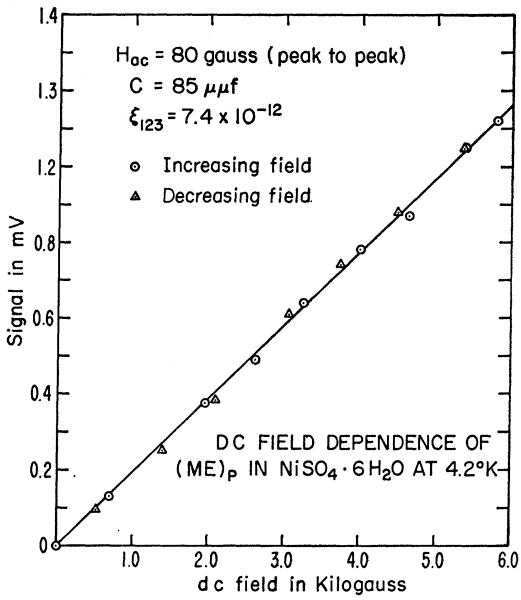

FIG. 3. Induced voltage as a function of H_{dc} parallel to the tetragonal axis in $NiSO_4 \cdot 6H_2O$ at 4.2°K. The modulation field, $h = \frac{1}{2}H_{ac} = 40$ G, is perpendicular to the c axis.

When the c axis of the crystal is parallel to H_{dc} and the modulation field h is at right angles, the measured voltage is

$$V_s = \xi \frac{H_c h A}{C_i+C_c} \cos\omega_m t\,.$$

This voltage is detected with a phase sensitive lock-in detector and a Texas Instrument recorder as shown in the block diagram of Fig. 2.

For $h = 40$ Oe amplitude, and $T = 4.2$°K the voltage is measured as a function of H_{dc} as shown in Fig. 3. The slope of the straight line corresponds to a value

$\xi(4.2°K) = 7.4 \times 10^{-12}$ erg $(G)^{-2}$ $(V/cm)^{-1}$ or

$$\xi(T = 4.2°K) = (2.2 \pm 0.2) 10^{-9} \text{ esu.}$$

The error of 10% includes the uncertainties in the measurement of the capacitances, the magnetic field and the electronic gain. The linearity with H_{dc} is expected to break down at very high fields in excess of 30 000 G as will be shown by the theoretical discussion in the following sections.

The effect cannot be ascribed to spurious pick-up, as was verified by a run with a dummy sample made of quartz. The very characteristic temperature dependence of the effect, shown by the experimental points in Fig. 4, will be explained theoretically by consideration of the magnetic energy levels of the Ni^{++} ions in this salt. At high temperatures, between 10 and 80°K, ξ goes approximately at T^{-2}. There is a pronounced maximum

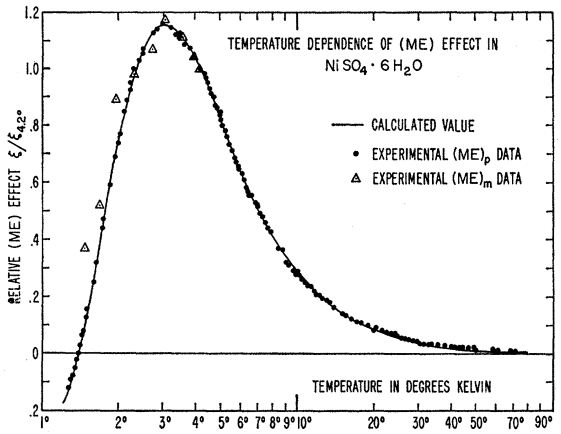

FIG. 4. Experimental temperature dependence of the PME effect. The black dots are obtained with the induced electric polarization. The triangles are obtained with an electrically induced magnetization.

near 3°K and ξ changes sign at 1.28°K. Theory predicts that ξ should reach an asymptotic value of -1.1×10^{-9} esu at absolute zero.

The effect also shows a characteristic dependence on the orientation of the crystal as is required by Eq. (2). The magnetic fields H_{dc} and h can be rotated around the vertical axis of the cryostat. The fields H_{dc} and h remain in the horizontal plane. The angle ϑ between H_{dc} and the horizontal tetragonal axis of the crystal is varied. The components of H_{dc} are consequently, $H_c = H_{dc}\cos\vartheta$, $H_a = H_{dc}\sin\vartheta\cos\varphi$ and $H_b = H_{dc}\sin\vartheta\sin\varphi$. The azimuth angle φ is fixed but arbitrary. When the modulation field $h\cos\omega_m t$ is perpendicular to H_{dc}, the electric polarization in the vertical direction is independent of φ and varies with ϑ. The induced signal is proportional to $\xi h H_{dc}\cos 2\vartheta\cos\omega_m t$. When the modulation field $h\cos\omega_m t$ is parallel to H_{dc}, the induced electric signal is proportional to $\xi h H_{dc}\sin 2\vartheta\cos\omega_m t$. These directional properties of the third-rank PME tensor for the

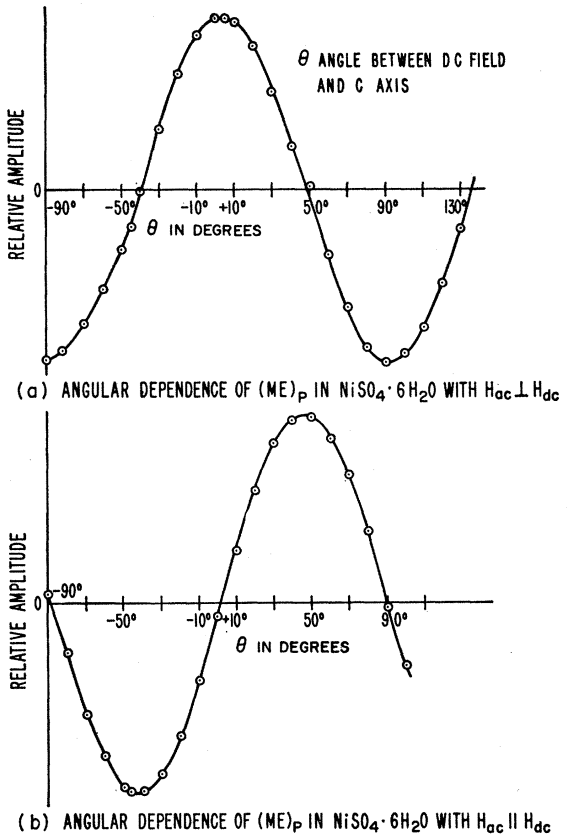

FIG. 5. Angular dependence of the induced electric polarization. The magnetic fields are in the horizontal plane and can be rotated around the vertical axis. The angle θ is the angle between H_{dc} and the horizontal c axis of the crystal.

D_4 symmetry are well verified by the experimental data shown in Fig. 5.

B. The Induced Magnetization Proportional to the Electric Field Strength

If an alternating voltage is impressed on the crystal shown in Fig. 1, an ac magnetization is induced at right angles to H_{dc}. This can in principle be detected by a pick-up voltage in the modulation coils. In practice this experiment proved to be much more difficult than the inverse effect described above. The experimental problems are threefold; breakdown due to a high voltage on the inner conductor of the coax line, increased sensitivity to spurious signals due to vibrations of highly charged conductors, and intrinsically low impedance level of the pick-up coils.

Therefore, another crystal holder assembly was constructed. Provision was made to evacuate the coax line and the sample holder to prevent gaseous breakdown. After evacuation a voltage with amplitude of 4000 V at 480 cps could be applied to a crystal about 8.5 mm thick. Contact with the crystal electrodes was made via phosphor bronze ribbons. Since the heat conduction to the sample was poor in the absence of the helium exchange

gas, the crystal was first cooled to the desired temperature. Then the heat-exchange gas was pumped out and then the high voltage was applied and a measurement made during 1 min.

A pick-up coil of 8000 turns was wound on the sample holder around the crystal inside the Dewar. The resistance of the coil was 2000 Ω at room temperature, but dropped to 20 Ω with $Q=30$ at liquid-helium temperature. The coil was tuned to 480 cps. An identical dummy coil was also mounted inside the Dewar. Their output was fed into a Keithley 103 push-pull preamplifier.

In spite of geometrical design precautions, the vibrations of the coils caused by the electrostatic force of the high-voltage leads produced a spurious pick-up voltage signal in the high magnetic field H_{dc}, equal to 20% of the true signal of the sample at 4.2°K. The signal has the same characteristic temperature dependence as the induced electric polarization. The experimental points are also shown in Fig. 4. The absolute magnitude of the signal was calibrated by comparison with the signal from a small coil of known self-inductance that replaced the crystal. The value of ξ thus obtained was 30% higher than that obtained previously. Because the former method is inherently more accurate, and can give all the physical information about the tensor ξ, no further data were obtained with the electrically induced magnetization.

III. THE MAGNETIC STRUCTURE OF $NiSO_4 \cdot 6H_2O$

A detailed review of the magnetic properties of $NiSO_4 \cdot 6H_2O$ has recently been given by Stout and Hadley.[11] Only the results that are most pertinent for the PME effect will be presented here. The crystal structure has been examined by Beevers and Lipson with x-ray techniques.[12] The point group symmetry is D_4 or 422. There are four Ni^{++} ions in the unit cell, each octahedrally coordinated with six H_2O molecules. The four Ni^{++} sites are related to each other by a rotation of $\pi/2$ around the c axis and a translation $\frac{1}{4}c$ along this screw axis. Each Ni^{++} site has C_2 symmetry. The twofold axis for sites I and III is along the [1,1,0] direction, for sites II and IV along [1,1̄,0].

The ground-state multiplet of the $3d^8$ electronic configuration of the Ni^{++} ion is ^3F. The dominant cubic-field component splits this multiplet into two triplets, T_{1g} and T_{2g}, and an orbital singlet A_{2g} which lies lowest. The separation between T_2 and A_2 is 10 $Dq \approx 8600$ cm^{-1}. The rhombic crystal field and the spin-orbit interaction $\lambda \mathbf{L}\cdot\mathbf{S}$ completely lift the remaining degeneracies. The orbital singlet ground state is therefore split into a spin triplet. According to Pryce[13] these spin states can be described by a spin Hamiltonian for $S=1$,

$$\mathcal{H}_s = -\lambda^2(\Lambda_x S_x^2+\Lambda_y S_y^2+\Lambda_z S_z^2) +\beta(g_x H_x S_x+g_y H_y S_y+g_z H_z S_z) -\beta^2(\Lambda_x H_x^2+\Lambda_y H_y^2+\Lambda_z H_z^2), \quad (3)$$

where

$$\Lambda_\alpha = \sum_i \frac{\langle 0|L_\alpha|i\rangle\langle i|L_\alpha|0\rangle}{W_i - W_0}, \quad (4)$$

and

$$g_\alpha = 2(1-\lambda\Lambda_\alpha). \quad (5)$$

The coordinate system has been chosen in such a manner to diagonalize the Λ tensor. The summation over all excited states $|i\rangle$ may be confined to the other states of the ^3F multiplet. The orbital angular momentum operator $\mathbf{L}$ transforms like T_1 and has only matrix elements connecting A_2 and T_2.

The spin Hamiltonian for $S=1$ in orthorhombic symmetry is often written in the form,

$$\mathcal{H}_s = D\{S_z^2-\tfrac{1}{3}S(S+1)\}+E(S_x^2-S_y^2) +\mathbf{S}\cdot\mathbf{g}\cdot\mathbf{H}+C. \quad (6)$$

Comparison of Eqs. (3) and (6) leads to the identification

$$C = -\tfrac{2}{3}\lambda^2(\Lambda_x+\Lambda_y+\Lambda_z) = -8\lambda^2/10Dq, \quad (7)$$

$$D = +\tfrac{1}{2}\lambda^2(\Lambda_x+\Lambda_y-2\Lambda_z), \quad (8)$$

$$E = -\tfrac{1}{2}\lambda^2(\Lambda_x-\Lambda_y). \quad (9)$$

In the absence of a magnetic field the eigenstates and eigenvalues of the spin Hamiltonian (6) are $W_0=-\frac{2}{3}D$ for $|s_z=0\rangle$, $W_1=\frac{1}{3}D-E$ for $2^{-1/2}\{|+1\rangle-|-1\rangle\}$ and $W_2=\frac{1}{3}D+E$ for $2^{-1/2}\{|+\rangle+|-\rangle\}$. The spin splittings have been most accurately determined from the low-temperature specific heat by Hadley and Stout,[11] $D=4.77$ cm^{-1}, $E=0.27$ cm^{-1}.

We have carried out a microwave-spin-resonance experiment at 30 kMc/sec. A broad resonance was observed at 77°K. The resonance occurs in a field of 6500±400 G parallel to the c axis and is 3500 G wide. It is presumably caused by a transition between the two upper levels. This resonance is not inconsistent with the crystal field splittings of Hadley and Stout, but the broad lines in this concentrated magnetic crystal impair the value of spin-resonance experiments.

The magnetic susceptibility of the ions in one kind of site, measured along the α axis of the orthorhombic ellipsoid, is given by

$$\chi_\alpha = -\frac{N}{H_\alpha}\left[\frac{1}{Z}\sum_{i=0}^{2}(\partial W_i/\partial H_\alpha)e^{-W_i/kT}\right]+2N\beta^2\Lambda_\alpha. \quad (10)$$

Here N^{-1} is the volume of the unit cell;

$$Z=\sum\exp(-W_i/kT)$$

is the partition function.

In relatively small magnetic fields, when the Zeeman

[11] J. W. Stout and W. B. Hadley, J. Chem. Phys. **40**, 55 (1964).
[12] C. A. Beevers and H. Lipson, Z. Krist. **83**, 123 (1932).
[13] M. H. L. Pryce, Proc. Roy. Soc. (London) **A214**, 237 (1952).

energy is small compared to the crystal field splitting, $g\beta H \ll D$ and E, the energy levels W_i can readily be determined by perturbation theory from the spin Hamiltonian (6). One finds,

$$\chi_x = \frac{2N\beta^2 g_x^2}{D-E} Z^{-1}\{1-e^{-(D-E)/kT}\} + 2N\beta^2\lambda^{-1}(1-\tfrac{1}{2}g_x), \quad (11a)$$

$$\chi_y = \frac{2N\beta^2 g_y^2}{D+E} Z^{-1}\{1-e^{-(D+E)/kT}\} + 2N\beta^2\lambda^{-1}(1-\tfrac{1}{2}g_y), \quad (11b)$$

$$\chi_z = \frac{2N\beta^2 g_z^2}{2E} Z^{-1}\{e^{-(D-E)/kT} - e^{-(D+E)/kT}\} + 2N\beta^2\lambda^{-1}(1-\tfrac{1}{2}g_z). \quad (11c)$$

Stout and Hadley[11] have derived from the observed magnetic anisotropy that the twofold axis at the Ni^{++} site cannot be the z axis. If this axis is chosen as the x direction, the z axis of the Λ tensor makes an angle $\phi = 40.2°$ with the tetragonal c axis. This value is consistent with the x-ray determination of the distorted octahedron of water moleculars surrounding the Ni^{++} ion.

Summation over the four different sites gives the macroscopic susceptibilities

$$\chi_c = 4(\chi_y \sin^2\phi + \chi_z \cos^2\phi),$$
$$\chi_a = \chi_b = 2\chi_x + 2\chi_y \cos^2\phi + 2\chi_z \sin^2\phi. \quad (12)$$

The magnetic susceptibility has been measured by Watanabe.[14] We have checked the temperature dependence of χ_a and χ_c. The experimental points are shown in Fig. 6. Good agreement with the drawn theoretical curves is obtained only if a correction for exchange between neighboring pairs of Ni^{++} ions is applied. In the effective field approximation this correction takes the form

$$\chi_{ex} = \frac{\chi}{1 - 2Jz\chi/Ng^2\beta^2}, \quad (13)$$

where χ is the uncorrected value given by Eqs. (11) and (12). The experimental data can be fitted with $2Jz = 0.42$ cm^{-1}. This exchange interaction leaves the specific-heat data above 1.5°K unchanged. The powder susceptibility at high temperatures gives an isotropic part of the g value, $\bar{g} = \frac{1}{3}(g_x + g_y + g_z) = 2.203 \pm 0.004$. From Eq. (5) the values $g_x = 2.216$, $g_y = 2.212$ and $g_z = 2.181$ are obtained if the spin-orbit coupling parameter $\lambda = -285$ cm^{-1} is used.

In the limit of very high magnetic fields the magnetic behavior is quite different. The eigenvalues W_i to be used in Eq. (10) must be determined from the diagonalization of the spin Hamiltonian matrix.

[14] T. Watanabe, J. Phys. Soc. Japan 17, 1856 (1962).

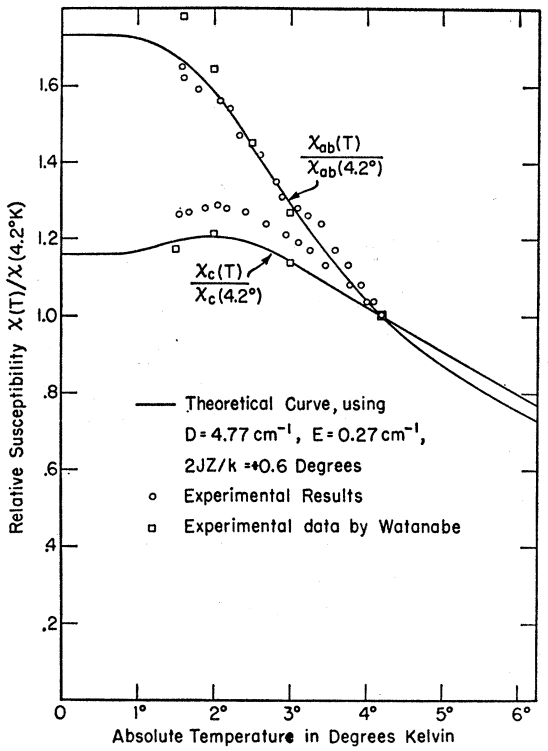

FIG. 6. The experimental data for the temperature dependence of the magnetic susceptibility are compared with the theoretical curve. A correction for spin exchange has been made.

Comparison of Figs. 4 and 6 shows the pronounced difference in the temperature dependence of χ and ξ. In the next section the spin Hamiltonian will be augmented by terms, which are linear functions of the applied electric field strength $\mathcal{E}$. This implies changes in the energy levels W_i and concomitant changes in the magnetic susceptibilities which are linear functions of $\mathcal{E}$.

IV. THEORY OF THE PME EFFECT

Since the Ni^{++} sites lack inversion symmetry, there will be components in the crystal-field potential with odd parity. This odd part of the potential V_{cr}^{u} will admix some odd parity configurations, such as $3d^7 4p$, to the $3d^8$ configuration. The admixture will be small because the $4p$ configuration is an estimated 60 000 cm^{-1} above the ^3F_g ground multiplet. This admixture may often be ignored, but it is of vital importance in the discussion of the magnetoelectric effects. The odd potential V_{cr}^{u} and the potential in an externally applied electric field $-e\,\mathcal{E}\cdot\mathbf{r}$ are simultaneously introduced into the perturbation calculation. If the usual perturbation calculation is carried out two steps farther with each of these odd terms used once, a part of the spin Hamiltonian is obtained which depends linearly on $\mathcal{E}$.

In the present example a linear variation of the Λ tensor with electric field is found,

$$\Delta_{\mathcal{E}}\Lambda_{kl} = \sum_j R_{jkl}\mathcal{E}_j.$$

The third-rank R tensor has components given by[10]

$$R_{jkl}=2\sum_{m,n,u}\frac{\langle {}^3A_{2g}|L_k|m\rangle\langle m|V_{cr}{}^u|u\rangle\langle u|-e\mathcal{E}_j r_j|n\rangle\langle n|L_l|{}^3A_{2g}\rangle}{(W_m-W_0)(W_n-W_0)(W_u-W_0)}. \tag{14}$$

Here W_0 is the energy of the orbital ground state ${}^3A_{2g}$, m and n are states of the ${}^3T_{2g}$ orbital triplet of the $3d^8\,{}^3F$ configuration, and u is a state with the opposite parity configuration $3d^74p$. The factor 2 is added because the real perturbations $V_{cr}{}^u$ and $-e\,\mathfrak{E}\cdot\mathbf{r}$ can be taken in different order. The energy levels retained in the summation of Eq. (14) produce the dominant contribution to R. The spin Hamiltonian is augmented by the terms

$$\mathfrak{IC}_{S,\mathcal{E}}=-\lambda^2\sum R_{jkl}\mathcal{E}_jS_kS_l-\lambda\beta\sum R_{jkl}\mathcal{E}_jS_kH_l -\beta^2\sum R_{jkl}\mathcal{E}_jH_kH_l. \tag{15}$$

The third-rank tensor may be symmetrized in the last two indices. Its elements are subjected to the symmetry requirements imposed by the site of the magnetic ion. For the C_2 symmetry of Ni^{++} ions with the x-axis as the twofold axis, the tensor takes the form

$$\begin{Vmatrix} R_{11} & R_{12} & R_{13} & R_{14} & 0 & 0 \\ 0 & 0 & 0 & 0 & R_{25} & R_{26} \\ 0 & 0 & 0 & 0 & R_{35} & R_{36} \end{Vmatrix}. \tag{16}$$

The Voigt notation has been used $R_{11}=R_{xxx}$, $R_{12}=R_{xyy}$, $R_{13}=R_{xzz}$ $R_{14}=R_{xyz}+R_{xzy}$, etc. The first three elements show that an electric field along the twofold axis changes the lengths of the principal axes of the Λ tensor. With the aid of Eqs. (7)–(9) the elements R_{11}, R_{12}, and R_{13} can be related to the variations of D, E and $10\,Dq$. The change in $10\,Dq$ is caused by a different shift in the energy levels ${}^2A_{2g}$ and ${}^3T_{2g}$ on the application of an electric field. The trace $R_{11}+R_{12}+R_{13}$ need not vanish.

$$\partial(10\,Dq)/\partial\mathcal{E}_x=-((10\,Dq)^2/12)(R_{11}+R_{12}+R_{13}). \tag{17}$$

$$\partial D/\partial\mathcal{E}_x=\{\tfrac{1}{2}(R_{11}+R_{12})-R_{13}\}\lambda^2. \tag{18}$$

$$\partial E/\partial\mathcal{E}_x=-\tfrac{1}{2}(R_{11}-R_{12})\lambda^2. \tag{19}$$

The variations of the g factors g_x, g_y, and g_z with the applied electric field follow from Eqs. (5) and (14). The expressions for the susceptibilities may now be differentiated with respect to $\mathcal{E}_x$ as follows,

$$\frac{\partial\chi_\alpha}{\partial\mathcal{E}_x}=\frac{\partial\chi_\alpha}{\partial g_\alpha}\frac{\partial g_\alpha}{\partial\mathcal{E}_x}+\frac{\partial\chi_\alpha}{\partial D}\frac{\partial D}{\partial\mathcal{E}_x}+\frac{\partial\chi_\alpha}{\partial E}\frac{\partial E}{\partial\mathcal{E}_x}. \tag{20}$$

The change in the susceptibility is expressed in terms of R_{11}, R_{12}, and R_{13} with Eqs. (17)–(19).

The remaining elements of the R tensor produce a rotation of the Λ tensor. Consider, for example, the element R_{14}. It describes a rotation in the zy plane around the x axis produced by $\mathcal{E}_x$. The magnitude of the rotation may be obtained from a rediagonalization of the Λ tensor

$$\begin{Vmatrix} \Lambda_x & 0 & 0 \\ 0 & \Lambda_y & R_{14}\mathcal{E}_x \\ 0 & R_{14}\mathcal{E}_x & \Lambda_z \end{Vmatrix}.$$

The tensor is rotated through an angle Θ_x given by

$$\tan2\Theta_x=2R_{14}\mathcal{E}_x/(\Lambda_z-\Lambda_y). \tag{21}$$

The change in the magnetic free energy caused by this rotation in the presence of a magnetic field is

$$-\tfrac{1}{2}(\chi_z-\chi_y)\sin2\Theta H_zH_y\approx-(\chi_z-\chi_y)\times(R_{14}/(\Lambda_z-\Lambda_y))\mathcal{E}_xH_yH_z.$$

There are similar terms corresponding to the rotations of the Λ tensor around the y and z axis involving the elements R_{25}, R_{26}, R_{35}, and R_{36}. When all these terms are collected for one type of Ni^{++} sites, the paramagnetoelectric free energy for the Ni^{++} ions on site I is found to be

$$\begin{aligned} F_{\mathrm{PME}}{}^I=&-\tfrac{1}{2}\sum_{\alpha=x,y,z}\left\{\frac{\partial\chi_\alpha}{\partial g_\alpha}\frac{\partial g_\alpha}{\partial\mathcal{E}_x}+\frac{\partial\chi_\alpha}{\partial D}\frac{\partial D}{\partial\mathcal{E}_x}+\frac{\partial\chi_\alpha}{\partial E}\frac{\partial E}{\partial\mathcal{E}_x}\right\}H_\alpha{}^2\mathcal{E}_x \\ &-((\chi_x-\chi_y)/(\Lambda_z-\Lambda_y))R_{14}\mathcal{E}_xH_yH_z \\ &-((\chi_x-\chi_z)/(\Lambda_x-\Lambda_z))(R_{25}\mathcal{E}_y+R_{35}\mathcal{E}_z)H_xH_z \\ &-((\chi_x-\chi_y)/(\Lambda_x-\Lambda_y))(R_{26}\mathcal{E}_y+R_{36}\mathcal{E}_z)H_xH_y. \end{aligned} \tag{22}$$

The explicit temperature dependence of the Λ and R tensor is expected to be small. This is certainly true at liquid-helium temperatures, where the lattice vibrations are frozen in their zero-point amplitudes. The temperature dependence of the observed effect is caused entirely by the susceptibilities and their derivatives in Eq. (22).

A summation over the four different Ni^{++} sites in the unit cell must still be performed. The orthorhombic coordinate systems at these sites are related to each other by rotations of $\frac{1}{2}\pi$ around the c axis. This tetragonal axis is at right angles to the x axis and makes an angle $\phi=40.2°$ with the z axis at each site. On summation various terms cancel and the only remaining terms in the paramagnetoelectric free-energy density of the crystal are those occurring in Eq. (2). The summation of Eq. (22) over the four sites and the substitution of Eqs. (17)–(19) finally yields the paramagnetoelectric constant occurring in the thermodynamic expression of

Eq. (2).

$$\begin{aligned}\xi=\sin 2\phi\{&[+f_D(T)+f_{gD}T](\tfrac{1}{2}R_{11}+\tfrac{1}{2}R_{12}-R_{13})\lambda^2\\&-[+f_E(T)+f_{gE}(T)](-\tfrac{1}{2}R_{11}+\tfrac{1}{2}R_{12})\lambda^2\\&+\tfrac{1}{12}f_{10Dq}(T)(10\,Dq)^2(R_{11}+R_{12}+R_{13})\}\\&+2\lambda^2\cos 2\phi f_A(T)R_{14}\\&+2\lambda^2\cos\phi f_B(T)(R_{25}\cos\phi-R_{35}\sin\phi)\\&+2\lambda^2\sin\phi f_C(T)(R_{26}\cos\phi-R_{36}\sin\phi)\,. \quad (23)\end{aligned}$$

The temperature-dependent functions are given by

$$\begin{aligned}f_D(T)&=+\partial\chi_y/\partial D-\partial\chi_z/\partial D,\\f_E(T)&=-\partial\chi_y/\partial E+\partial\chi_z/\partial E,\\f_{gD}(T)&=-(2/3\lambda)(\partial\chi_y/\partial g_y+2(\partial\chi_z/\partial g_z)),\\f_{gE}(T)&=-(2/\lambda)(\partial\chi_y/g_y)\,, \quad (24)\\f_A(T)&=+(\chi_z-\chi_y)/(D-E)\,,\\f_B(T)&=-(\chi_x-\chi_z)/(D+E)\,,\\f_C(T)&=(\chi_x-\chi_y)/2E,\\f_{10Dq}(T)&=-(8\lambda/(10Dq)^2)(\partial\chi_y/\partial g_y-\partial\chi_z/\partial g_z)\,.\end{aligned}$$

In the weak-magnetic-field approximation the susceptibilities are given by Eqs. (11) and the temperature dependence is readily calculated. The dominant terms at low temperature are $f_D(T)$ and $f_E(T)$. The second-order temperature-independent paramagnetic terms in Eqs. (11) are ignored. The small anisotropy in the g values may likewise be neglected for our purposes.

$$\begin{aligned}f_D(T)=-2N\bar{g}^2\beta^2\Bigg\{&\frac{1-e^{-(D+E)/kT}}{Z(D+E)^2}-\frac{1}{Z^2kT}\\&\times\Bigg[\frac{e^{-(D-E)/kT}+2e^{-(D+E)/kT}}{D+E}\\&+\frac{e^{-(D-E)/kT}-e^{-(D+E)/kT}}{2E}\Bigg]\Bigg\},\end{aligned}$$

$$\begin{aligned}f_E(T)=2N\bar{g}^2\beta^2\Bigg\{&+\frac{1-e^{-(D+E)/kT}}{Z(D+E)^2}\\&\times\frac{e^{-D/kT}\left(1-\dfrac{3E}{kT}+2e^{-D/kT}\right)}{Z^2kT(D+E)}\Bigg\}.\end{aligned}$$

In the limit of high temperature, one has $f_D(T)=f_E(T)=2N\bar{g}^2\beta^2/6k^2T^2$. At $T=0$°K they have the asymptotic values

$$+f_D(T=0)=-\frac{2N\bar{g}^2\beta^2}{(D+E)^2},\quad f_E(T=0)=\frac{2N\bar{g}^2\beta^2}{(D+E)^2}.$$

The function $f_D(T)$ changes sign near 2.5°K.

The functions f_{gD} and f_{gE} are smaller by a factor $(D+E)\lambda^{-1}\approx 10^{-2}$ at low temperature. At high temperature they vanish as T^{-1}, $3f_{gD}=-f_{gE}=8N\bar{g}^2\beta^2/\bar{g}\lambda kT$. The experimental data show that the contribution of terms proportional to T^{-1} in the PME effect are quite small. They have their origin in a variation of the $\bar{g}$ value with electric field. Even near 50°K the T^{-2} dependence due to the variation of the crystal field splittings dominates the PME effect. The theoretical temperature variations of $F_D=f_D+f_{gD}$ and $F_E=f_E+f_{gE}$ are plotted in Fig. 7.

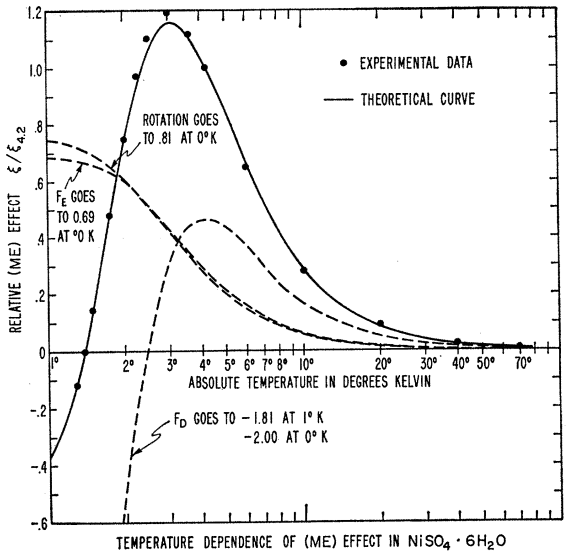

FIG. 7. Comparison between theory and experiment of the temperature dependence of the PME effect in $NiSO_4 \cdot 6H_2O$.

Since $\partial\chi_y/\partial g_y-\partial\chi_z/\partial g_z\approx 2(\chi_x-\chi_z)/\bar{g}$, the temperature dependence of f_{10Dq} is essentially the same as f_A. The anisotropic susceptibilities $f_B(T)$ and $f_C(T)$ have essentially the same temperature dependence. Therefore a single function $f_R(T)=\frac{1}{3}\{f_A(T)+f_B(T)+f_C(T)\}$ is plotted in Fig 7 to describe the effect of rotations. The contribution of the term in f_{10Dq} is smaller by a factor $(D-E)\lambda^{-1}$ than the rotational terms at low temperatures.

The three functions $F_D(T)$, $F_E(T)$ and $F_R(T)$ in Fig. 7 have been multiplied by appropriate weight factors in such a manner that their sum represented by the full drawn curve approximates closely the experimentally observed temperature dependence of ξ. The microscopic theory gives a satisfactory explanation of this striking behavior. The sign reversal at low temperature is due to the variation of D with electric field. The best fit with the experimental data is obtained for the following values of coefficients in Eq. (23),

$$(\tfrac{1}{2}R_{11}+\tfrac{1}{2}R_{12}-R_{13})\lambda^2=7.86\times10^{-8}\ \text{cm}^{-1}/\text{V/cm}\,, \quad (25)$$

$$-\tfrac{1}{2}(-R_{11}+R_{12})\lambda^2=+2.60\times10^{-8}\ \text{cm}^{-1}/\text{V/cm}\,, \quad (26)$$

$$\begin{aligned}&-(4/3\bar{g})(D-E)\lambda(R_{11}+R_{12}+R_{13})+2\cot(2\phi)\lambda^2R_{14}\\&\quad+\lambda^2\sin\phi(R_{25}\cos\phi-R_{36}\sin\phi)\\&\quad+\lambda^2\cos\phi(R_{35}\cos\phi-R_{36}\sin\phi)\\&\quad=+2.5\times10^{-8}\ \text{cm}^{-1}/\text{V/cm}. \quad (27)\end{aligned}$$

Since the temperature dependence of $f_E(T)$ and $f_R(T)$ is quite similar according to Fig. 7, the individual contributions of Eqs. (26) and (27) are not easily separable. Only their sum has a precise meaning. The relative

variation of the crystal field splitting D is quite well determined from Eq. (25),

$$|(1/D)(\partial D/\partial \mathcal{E}_x)| = (1.65 \pm 0.15) \times 10^{-8}/\text{V/cm}.$$

V. DISCUSSION

This variation is in good agreement with the order-of-magnitude estimate of the effect before its discovery, as was discussed in the introduction of this paper. The absolute sign has not been determined. This would require the determination of the absolute configuration of the atoms in the unit cell. The two piezoelectric types, related to each other by the inversion operation, would have opposite sign for ξ as well as for the piezoelectric constant.

The piezoelectric properties entail the existence of a piezoelectric strain. The whole discussion has so far ignored the deformation of the unit cell and has been concerned with the paramagnetoelectric effect at constant strain, while the experimental effect is observed under constant stress. Another measurement involving the effect of strain on the magnetic susceptibility would be necessary to relate the two quantities. From the general observations of the influence of the electric field on spin resonance spectra,[15] it may be inferred that the effect of piezoelectric strain is usually only a few percent, or less, of the effect of an electric field at constant strain on any parameter in the spin Hamiltonian. We assume this to be the case also for $NiSO_4 \cdot 6H_2O$. The over-all temperature dependence of the observed effect is dominated by the variation of D with electric field.

In principle, other relationships, besides Eqs. (25)–(27), between the elements of the R tensor might be obtained by measuring the temperature dependence of the effect in intermediate and very high magnetic fields. For each value and orientation of a large dc magnetic field the three spin energy levels and eigenfunctions of the Ni^{++} ion and their variation with electric field may in principle be determined from the spin Hamiltonian (6) and (15). From Eq. (10) the variation of the paramagnetic susceptibility follows. In practice, only the limiting case of very large magnetic fields $g\beta H \gg D$ is readily accessible to analysis. The PME effect becomes quite small in high fields for the symmetry of $NiSO_4 \cdot 6H_2O$, but not necessarily for other symmetries.

The PME effect has typical nonlinear characteristics, as it is described by a free energy which is cubic in the field amplitudes. If two applied fields are both modulated at different frequencies, a polarization at the sum and difference frequency will be induced. It has of course been assumed that the modulation frequency is small compared to the relaxation rate. The PME effect will show dispersion from the isothermal values calculated in this paper, when the modulation frequencies are comparable with the inverse relaxation times.

The microscopic basis of the PME effect is essentially the same as for the magnetoelectric (ME) effect in antiferromagnetic Cr_2O_3, as proposed by Rado.[16] The absence of cooperative phenomena and domains makes a detailed theoretical interpretation more amenable in the paramagnetic case. The paramagnetic phase of Cr_2O_3 shows no effect, because it has a center of inversion. The temperature dependence of the ME effect in antiferromagnetic Cr_2O_3 is not completely clarified. There is a sign reversal at low temperature, which may have its origin in a dependence of the exchange integral J between a pair of Cr^{3+} ions on the applied electric field. This interaction was proposed by Date[17] and has been discussed by Pratt.[18] The electric-field dependence of the exchange interaction may also be important in the ME effect of the weakly ferromagnetic piezoelectric crystal of gallium ferrite.[19]

In the case of $NiSO_4 \cdot 6H_2O$ the paramagnetic susceptibility at low temperature is somewhat influenced by the exchange interaction between Ni^{++} ions, as shown in Eq. (13). If this expression is differentiated with respect to the applied electric field, one obtains an exchange correction for the PME effect,

$$\frac{\partial \chi_{ex}}{\partial \mathcal{E}} = \frac{(\partial \chi/\partial \mathcal{E}) + \chi^2 (2zNg^2\beta^2)(\partial J/\partial \mathcal{E})}{[1-(2Jz/Ng^2\beta^2)\chi]^2}.$$

Since the exchange correction on the susceptibility is less than 30% down to 1.5°K, the exchange correction on the over-all temperature dependence of the PME effect is relatively small. The relative contributions of the terms in $f_E(T)$ and $f_R(T)$ in Fig. 7 and Eqs. (26) and (27) may require a considerable correction. The various contributions to the PME effect cannot be unraveled from the measurement of $\xi(T)$ alone. A good idea of the importance of $\partial J/\partial \mathcal{E}$ could be obtained from the electric shift of magnetic resonance spectra of ion pairs. This experiment should be feasible in ruby, but electron spin resonance in $NiSO_4 \cdot 6H_2O$ is not informative because of the excessive linewidth.

The microscopic origin of the PME effect appears to be well established by the excellent agreement obtained for the striking temperature dependence in $NiSO_4 \cdot 6H_2O$. This first successful example should encourage investigation of other piezoelectric paramagnetic crystals. A crystal that would be amenable to a similar investigation is the isomorphous $NiSeO_4 \cdot 6H_2O$. The PME effect should occur equally well for rare-earth ions. An example of a piezoelectric crystal including these ions is $Nd(BrO_3)_3 \cdot 9H_2O$.

ACKNOWLEDGMENTS

The authors are indebted to Dr. S. Foner for his advice on the design of the apparatus, which was skillfully built by E. Johnson.

[15] See Refs. 8 and 9.

[16] See Ref. 10.

[17] M. Date, J. Kanamori, and M. Tachiki, J. Phys. Soc. Japan **16**, 2589 (1961).

[18] T. Izuyama and G. W. Pratt, J. Appl. Phys. **34**, 1226 (1963).

[19] G. T. Rado, Phys. Rev. Letters **13**, 335 (1964).